View metadata, citation and similar papers at core.ac.uk
brought to you by CORE
provided by Xiamen University Institutional Repository

The Journal of Physical Chemistry Letters
Letter
Cite This: J. Phys. Chem. Lett. 2019, 10, 5868−5872
pubs.acs.org/JPCL

Two-Dimensional Analysis of the Diabatic Transition of a General Vectorial Physical Observable Based on Adiabatic-to-Diabatic Transformation

Mingxing Ren,[†] Bo Ma,[†] Zhenhua Chen,[*,†] and Wei Wu[‡]

[†]Fujian Provincial Key Laboratory of Theoretical and Computational Chemistry and College of Chemistry and Chemical Engineering, Xiamen University, Xiamen, Fujian 361005, China

[‡]The State Key Laboratory of Physical Chemistry of Solid Surfaces, iChem, and College of Chemistry and Chemical Engineering, Xiamen University, Xiamen, Fujian 361005, China

Supporting Information

ABSTRACT: We present a full analysis of the magnitude and orientation of the diabatic transition matrix element of a general vectorial physical observable during the adiabatic-to-diabatic transformation. The diabatic transition is a function of the adiabatic-to-diabatic transformation angle and the two basic vectors of the adiabatic states, which are the off-diagonal matrix element and the difference between the two diagonal matrix elements. To the best of our knowledge, this is the first time that the transformation has been accomplished in a more general two-dimensional scale for a vectorial physical observable. All possible extreme values of a diabatic transition are deduced for systems with different features. By using an approximate diabatic transition dipole, the pilot implementation of the analysis produces an electronic coupling curve nearly identical to that obtained by the generalized Mulliken−Hush method for the testing molecule. Evidently, this complete analysis of a diabatic transition will be very useful in determining the adiabatic-to-diabatic transformation angle by using a physical observable and can also be used to evaluate the quality of various approximations for constructing the diabatic states.

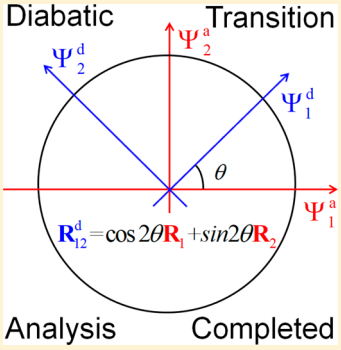

The nonadiabatic process is playing a more important role in the exploration of the electron and energy transfer reactions in many solar energy materials,[1−4] laser-driven chemistry,[5−10] and even biological systems.[11−13] Quantum mechanically, it can be studied either in adiabatic or in diabatic representation.[14−16] Although these two representations are equivalent and can be transformed mutually via a unitary matrix, diabatic representation is often more convenient for use in nonadiabatic processes. Computationally, adiabatic representation has the advantage in that the adiabatic states can be evaluated directly by standard electronic structure methods. This inspires an indirect diabatization scheme, in which one deduces the adiabatic representation first and then transforms it to the diabatic one.[17−19] Meanwhile, the diabatic states can also be constructed straightforwardly by some theoretical methods such as configurational uniformity,[20,21] constrained density functional theory,[22,23] valence bond theory,[24,25] etc. In addition, one can also investigate the nonadiabatic process via means of direct computation of nonadiabatic coupling.[26,27]

In general, the indirect diabatization scheme is effortless for implementation and can be feasibly accomplished. Moreover, satisfactory results with acceptable accuracy can often be obtained, especially when an auxiliary physical observable assists in the transformation. Over the years, a large number of methods have been proposed along this line.[28−35] Of the observables, vector quantities have attracted a great deal of attention, among which the dipole moment[28−32,36−39] has been the most extensively investigated. In general terms, both the magnitude and the direction of the vector quantity would contribute to the adiabatic-to-diabatic transformation. However, to the best of our knowledge, the direction of the auxiliary observable has never been taken into consideration in the literature. In this work, we perform a rigorous and complete analysis of the diabatic transition for a most general vector physical observable.

First, without a loss of generality, let us assume that we have a set of adiabatic states ($\mathbf{\Psi}^a$) in the adiabatic representation and a set of diabatic states ($\mathbf{\Psi}^d$) in the diabatic representation. These two sets of wave functions span the same space and can be transformed mutually by a unitary matrix ($\mathbf{U}$)

$$\mathbf{\Psi}^a = \mathbf{\Psi}^d\mathbf{U} \text{ and } \mathbf{\Psi}^d = \mathbf{\Psi}^a\mathbf{U}^+ \tag{1}$$

Specifically, for the two-state model, the unitary matrix can be parametrized by a transformation angle (θ) as

$$\mathbf{U} = \begin{pmatrix} \cos\theta & -\sin\theta \\ \sin\theta & \cos\theta \end{pmatrix} \tag{2}$$

Received: June 23, 2019
Accepted: September 15, 2019
Published: September 16, 2019

ACS Publications © 2019 American Chemical Society

DOI: 10.1021/acs.jpclett.9b01812
J. Phys. Chem. Lett. 2019, 10, 5868−5872

Downloaded via XIAMEN UNIV on February 24, 2020 at 01:24:02 (UTC).
See https://pubs.acs.org/sharingguidelines for options on how to legitimately share published articles.

where θ is confined in the region from $-\pi/4$ to $\pi/4$, to keep the difference between the adiabatic and diabatic bases as small as possible.

For a physical quantity ($\mathbf{R}$), it can be expressed in matrix form either in an adiabatic representation or in a diabatic one with the matrix elements as

$$\mathbf{R}^{\mathrm{a}}_{ij} = \langle \mathbf{\Psi}^{\mathrm{a}}_i | \mathbf{R} | \mathbf{\Psi}^{\mathrm{a}}_j \rangle \text{ and } \mathbf{R}^{\mathrm{d}}_{ij} = \langle \mathbf{\Psi}^{\mathrm{d}}_i | \mathbf{R} | \mathbf{\Psi}^{\mathrm{d}}_j \rangle \tag{3}$$

We should note that the matrix elements, which store different components of the quantity, are also vectors rather than scalars in the usual matrix analysis. Within the two-state framework, because the diabatic and adiabatic states can be transformed mutually, the transition in the diabatic presentation ($\mathbf{R}^{\mathrm{d}}_{12}$) can be expressed as

$$\mathbf{R}^{\mathrm{d}}_{12} = \langle \mathbf{\Psi}^{\mathrm{d}}_1 | \mathbf{R} | \mathbf{\Psi}^{\mathrm{d}}_2 \rangle = \cos 2\theta \mathbf{R}_1 + \sin 2\theta \mathbf{R}_2 \tag{4}$$

where $\mathbf{R}_1$ denotes the transition in adiabatic presentation

$$\mathbf{R}_1 = \mathbf{R}^{\mathrm{a}}_{12} \tag{5}$$

and $\mathbf{R}_2$ is the difference in the quantity

$$\mathbf{R}_2 = \frac{1}{2}(\mathbf{R}^{\mathrm{a}}_{22} - \mathbf{R}^{\mathrm{a}}_{11}) \tag{6}$$

Obviously, $\mathbf{R}^{\mathrm{d}}_{12}$ is a function of the two basic vectors $\mathbf{R}_1$ and $\mathbf{R}_2$ and transformation angle θ. Equation 4 is the central equation of the paper. It provides a roundabout way to deduce the diabatic transition from the transformation angle, provided that we have already obtained the adiabatic quantities either experimentally or theoretically. Similarly, for a given diabatic transition, the transformation angle can be determined by using the adiabatic information. Consequently, eq 4 may play the key role in the adiabatic-to-diabatic transformation. According to the magnitudes and the angle (α) between the two basic vectors, we have three special cases (1−3) and the most common one to discuss about the orientation and magnitude of the diabatic transition.

Case 1. One of the basic vectors has a vanishing magnitude, i.e., $R_1 = 0$ or $R_2 = 0$. In this simplest case, eq 4 reduces to

$$\mathbf{R}^{\mathrm{d}}_{12} = \sin 2\theta \mathbf{R}_2 \text{ for } R_1 = 0 \tag{7a}$$

or

$$\mathbf{R}^{\mathrm{d}}_{12} = \cos 2\theta \mathbf{R}_1 \text{ for } R_2 = 0 \tag{7b}$$

Obviously, in this case, the trajectory of the diabatic transition is located on the same line as the non-zero basic vector, because the vanishing vector has no effect on the transition. Meanwhile, the magnitude of the diabatic transition is narrowed by a factor of $\sin 2\theta$ or $\cos 2\theta$ for vanishing $\mathbf{R}_1$ or $\mathbf{R}_2$, respectively.

From eq 4, we see that the diabatic transition quantity depends not only on the magnitudes of the two basic vectors $\mathbf{R}_1$ and $\mathbf{R}_2$ but also on the angle α between them. To this end, we classify the situations according to the different α values. In case 2, the two basic vectors are collinear. In case 3, they are perpendicular. The most general one is true for case 4.

Case 2. The two basic vectors are collinear, i.e., $\alpha = 0, \pi$. In this case, eq 4 reduces to

$$\mathbf{R}^{\mathrm{d}}_{12} = \sqrt{{R_1}^2 + {R_2}^2} \cos 2(\theta - \varphi) \cdot (\mathbf{R}_1/R_1) \tag{8}$$

where we have set the direction of $\mathbf{R}_1$ as a reference, and

$$\varphi = \cos \alpha \times \frac{1}{2} \arctan(R_2/R_1) \tag{9}$$

The magnitude and direction of $\mathbf{R}^{\mathrm{d}}_{12}$ are characterized by $\mathbf{R}_1$ and $\mathbf{R}_2$ as shown in Figure 1. Without a loss of generality, we

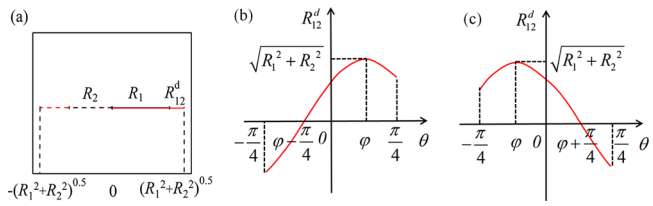

Figure 1. (a) Trajectory and magnitude of the diabatic transition $\mathbf{R}^{\mathrm{d}}_{12}$ as the adiabatic-to-diabatic transformation angle (θ) varies for collinear basic vectors ($\mathbf{R}_1//\mathbf{R}_2$). The negative value of R^{d}_{12} denotes that the transition is in the opposite direction as reference vector $\mathbf{R}_1$. The maximum of the transition can be achieved when θ is equal to φ, which may be either (b) positive when $\mathbf{R}_1$ and $\mathbf{R}_2$ are in the same direction or (c) negative for opposite directions.

assume that the magnitude of $\mathbf{R}^{\mathrm{d}}_{12}$ is located in a region [$T_{\min}$, $T_{\max}$]. From eq 8, it is obvious that $T_{\max} = \sqrt{{R_1}^2 + {R_2}^2}$, for $\theta = \varphi$. Meanwhile, the diabatic transition vanishes when $\theta = \varphi \pm \pi/4$. It is interesting to mention here that on the basis of the assumption of a vanishing diabatic transition dipole, the generalized Mulliken−Hush method (GMH) has been effectively developed for electronic coupling calculation.[29] However, it should be noted that a vanishing diabatic transition is valid only for this special case in which the two basic vectors $\mathbf{R}_1$ and $\mathbf{R}_2$ are collinear or for a scalar quantity that does not have direction at all. In general, the diabatic transition cannot always take a vanishing value for vector quantities, as we will see in the following cases.

Case 3. The two vectors $\mathbf{R}_1$ and $\mathbf{R}_2$ are mutually perpendicular, i.e., $\alpha = \pi/2$. This is the last special case. In this case, we set up a Cartesian coordinate system with the directions of $\mathbf{R}_1$ and $\mathbf{R}_2$ as x and y axes, respectively (see Figure 2). Now, the coordinate of the diabatic transition can be expressed as

$$\begin{cases} x = R_1 \cos 2\theta \\ y = R_2 \sin 2\theta \end{cases} \tag{10}$$

From eq 10, we see that the trajectory of the diabatic transition forms an ellipse when the transformation angle varies. Figure 2 plots the trajectory and the magnitude as a function of θ. It shows that the long axis of the ellipse is on the $\mathbf{R}_1$, when $R_1 > R_2$; meanwhile, it is on R_2, for $R_1 < R_2$. In the case that $R_1 = R_2$, the ellipse reduces to a circle. From eq 10, the magnitude of the diabatic transition can be expressed as

$$\mathbf{R}^{\mathrm{d}}_{12} = ({R_1}^2 \cos^2 2\theta + {R_2}^2 \sin^2 2\theta)^{1/2} \tag{11}$$

For $R_1 = R_2$, because the ellipse reduces to a circle, the magnitude becomes a constant with a value that is the same as R_1, no matter what values the transformation angle takes. When $R_1 > R_2$, however, the magnitude has its maximum $T_{\max} = R_1$, when θ is equal to zero, and takes its minimum $T_{\min} = R_2$ for $\theta = \pm\pi/4$. Similarly, when $R_1 < R_2$, the maximum $T_{\max} = R_2$ can be reached for $\theta = \pm\pi/4$ and the minimum $T_{\min} = R_1$ is located at $\theta = 0$.

In general, the magnitude of the diabatic transition can take a value only within the region from min(R_1, R_2) to max(R_1,

DOI: 10.1021/acs.jpclett.9b01812
J. Phys. Chem. Lett. 2019, 10, 5868−5872

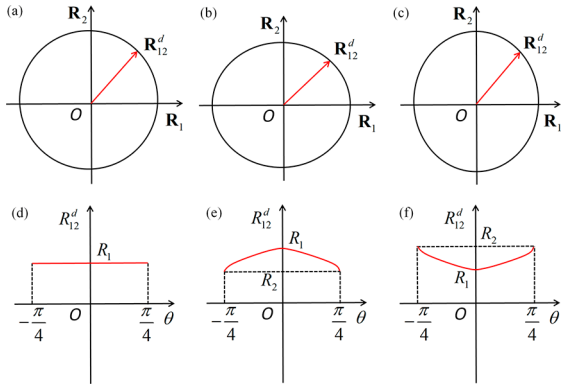

Figure 2. Trajectory and the magnitude of $\mathbf{R}_{12}^{\mathrm{d}}$ for mutually perpendicular basic vectors ($\mathbf{R}_1 \perp \mathbf{R}_2$). The trajectory forms (a) a circle for $R_1 = R_2$ or (b and c) an ellipse for $R_1 > R_2$ or $R_1 < R_2$. The magnitude becomes (d) a constant when $R_1 = R_2$ and takes values from $\min(R_1, R_2)$ to $\max(R_1, R_2)$ for (e) $R_1 > R_2$ and (f) $R_1 < R_2$.

R_2), when the two basic vectors are perpendicular. As we have mentioned in case 2 by forcing the diabatic transition to take the vanishing extreme, some diabatization schemes might be developed for two parallel basic vectors and for a scalar physical observable. However, for vector observables, a similar strategy may be not adequate, inasmuch as the minimum might always be larger than zero.

In fact, when the two basic vectors are perpendicular, minimizing or maximizing the diabatic transition cannot provide a useful diabatization scheme, because there are no extreme values at all for $R_1 = R_2$ or the extreme values are reached when the adiabatic and diabatic bases coincide with each other for a vanishing transformation angle or at the trivial diabatic basis with a transformation angle equal to $\pm\pi/4$. Therefore, if we are concerned about the accuracy of the diabatic quantities, e.g., electronic coupling, it turns out that we should take into consideration both the magnitudes and directions of the two basic vectors. In the next case, we will further discuss the property of the diabatic transition for the most general situation, in which angle α takes no special values.

Case 4. Vectors $\mathbf{R}_1$ and $\mathbf{R}_2$ form an oblique coordinate system. For the sake of clarity, in this case, it is still more convenient to establish a rectangular coordinate system. Here, $\mathbf{R}_1$ is taken as the x axis, and the y axis is set perpendicular to it. Then the trajectory of the diabatic transition is parametrically represented as

$$\begin{cases} x = R_1 \cos 2\theta + R_2 \sin 2\theta \cos \alpha \\ y = R_2 \sin 2\theta \sin \alpha \end{cases} \tag{12}$$

The trajectory is certainly a quadratic curve. To further identify the curve, we first perform a coordinate transformation by using a unitary matrix ($\mathbf{T}$). The coordinates in the new coordinate system are obtained by rotating the old one as

$$(\mathbf{x}'\mathbf{y}') = (\mathbf{xy})\mathbf{T} \tag{13}$$

where transformation $\mathbf{T}$ is expressed in terms of the angle γ as

$$\mathbf{T} = \begin{pmatrix} \cos\gamma & \sin\gamma \\ -\sin\gamma & \cos\gamma \end{pmatrix} \tag{14}$$

It can be proved that by taking angle γ as

$$\cot 2\gamma = \frac{R_1^2 + R_2^2 \cos 2\alpha}{R_2^2 \sin 2\alpha} \tag{15}$$

in the new Cartesian coordinate system, eq 12 will reduce to a standard equation of an ellipse

$$\begin{cases} x' = a \cos 2(\theta + \beta) \\ y' = b \sin 2(\theta + \beta) \end{cases} \tag{16}$$

where

$$a^2 = \frac{1}{2}(R_1^2 + R_2^2) + \frac{1}{2}\sqrt{(R_1^2 + R_2^2)^2 - 4R_1^2R_2^2 \sin^2\alpha} \tag{17}$$

$$b^2 = \frac{1}{2}(R_1^2 + R_2^2) - \frac{1}{2}\sqrt{(R_1^2 + R_2^2)^2 - 4R_1^2R_2^2 \sin^2\alpha} \tag{18}$$

$$\beta = \frac{1}{4}\arctan\frac{2R_1R_2\cos\alpha}{R_1^2 - R_2^2} \tag{19}$$

Equation 16 shows that the trajectory of the diabatic transition forms an ellipse when θ varies, similar to case 3. As shown in Figure 3, the major and minor axes of the ellipse are

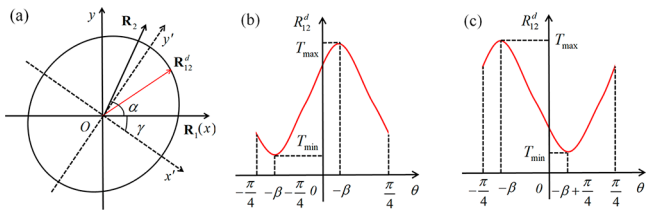

Figure 3. Trajectory and magnitude of $\mathbf{R}_{12}^{\mathrm{d}}$ for the most general case. (a) A clockwise rotation of the coordinate system by an angle of γ produces a standard ellipse equation for the trajectory. (b) $\beta < 0$. (c) $\beta > 0$.

on the x' and y' axes, respectively. After some deductions, the magnitude of $\mathbf{R}_{12}^{\mathrm{d}}$ can be expressed as a function of θ as

$$\mathbf{R}_{12}^{\mathrm{d}} = \left[\frac{1}{2}(R_1^2 + R_2^2) + \frac{1}{2}\cos 4(\theta + \beta) \sqrt{(R_1^2 + R_2^2)^2 - 4R_1^2R_2^2 \sin^2\alpha}\right]^{1/2} \tag{20}$$

Figure 3 plots $\mathbf{R}_{12}^{\mathrm{d}}$ versus θ. For the sake of convenience, we assume that the magnitude of the diabatic transition ranges from $T_{\min}$ to $T_{\max}$, which depend on the angle α between the two basic vectors. It is evident that the magnitude has its maximum $T_{\max} = a$ for $\theta = -\beta$. Meanwhile, the minimum ($T_{\min} = b$) is reached when $\theta = -\beta \pm \pi/4$. As we showed in the previous case, the direction can be of equal importance for vector quantity. In this case, we see clearly that the angle α contributes explicitly to the diabatic transition. Therefore, eq 20 illustrates that one would need to take into account the direction together with the magnitude to evaluate the diabatic transition correctly.

We note that for the special cases (i.e., $\alpha = 0$, $\pi/2$, and π), we can simply set γ in eq 15 to 0 as there are no needs to transform the coordinate system. From eq 20, we see that when $\alpha = 0$, π, the magnitude of $\mathbf{R}_{12}^{\mathrm{d}}$ will decrease to the region in case 2 in which the two basic vectors are collinear. In the case of perpendicular basic vectors, the magnitude falls in the

DOI: 10.1021/acs.jpclett.9b01812
J. Phys. Chem. Lett. 2019, 10, 5868−5872

region from min(R_1, R_2) to max(R_1, R_2), which will turn into case 3.

To accomplish the adiabatic-to-diabatic transformation, we would need not only the information about the adiabatic states but also the diabatic transition quantity. Here, we present a very simple approach, as the pilot application of the aforementioned analysis, by using the dipole moment. To obtain the adiabatic-to-diabatic transformation angle, we use an approximate diabatic transition dipole moment (see the Supporting Information for more details). The difference $\boldsymbol{\sigma}(\theta)$ between the approximate diabatic transition dipole moment $\mathbf{R}_{12}^{\sim d}$ and the transforming one in eq 4 is written as

$$\boldsymbol{\sigma}(\theta) = \mathbf{R}_{12}^{\sim d} - \mathbf{R}_{12}^{d} = \mathbf{R}_{12}^{\sim d} - \cos 2\theta \mathbf{R}_1 - \sin 2\theta \mathbf{R}_2 \quad (21)$$

Apparently, $\boldsymbol{\sigma}(\theta)$ is a function of the transformation angle. By minimizing the length of the $\boldsymbol{\sigma}$ vector, we have the transformation angle.

As an illustrative exemplification, we use both the novel approach and GMH method to explore the electron transfer between the two methylene groups in the equatorial−equatorial conformers of 1,3-dimethylenecyclohexane radical anion (see Scheme 1). Figure 4 plots the curves of various quantities for this molecule as the selected dihedral angle (ω) changes. Interestingly, it can be seen from Figure 4d that this novel approach and GMH method produce nearly identical electronic coupling curves, with differences of <5 meV. Presumably, there are two reasons. First, the diabatic transition dipoles are very smaller along the whole path (see Figure 4b). Secondarily, for the testing molecule, the directions of the two basic vectors are near collinear or one of the two basic vectors is close to zero (see Figure 4a). Consequently, GMH method becomes an effective approach for approximating the diabatic states as the basic assumption of the vanishing diabatic transition dipole is nearly satisfied. Nevertheless, the novel approach would be considered to be more adequate in the case in which the transition dipole is non-negligible, and the two basic vectors have comparable lengths together with a considerable angle α. One of the major goals in our future investigation of the novel approach is to determine the systems for which these two factors are simultaneously effective.

Scheme 1. Self-Exchange Electron Transfer between the Two Equatorial Lying Methylene Groups in 1,3-Dimethylenecyclohexane Radical Anion[a]

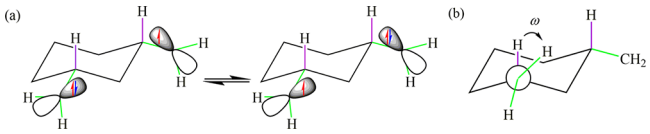

[a]One of the methylene groups is allowed to rotate rigidly by a torsional angle of ω to define different conformations of the model molecule.

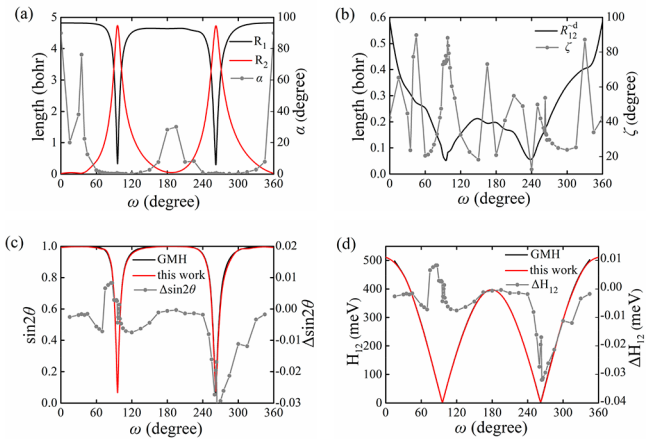

Figure 4. Curves of various quantities for the testing molecule as the selected dihedral angle (ω) changes: (a) magnitudes of the adiabatic basic vectors and the angle α between them, (b) magnitude of approximate diabatic transition dipole R_{12} and the angle ζ between it and the R_1 vector, (c) sin 2θ values, and (d) electronic coupling element H_{12} evaluated by GMH and the novel method, along with their differences.

In summary, we have derived a close equation (eq 4) for the transition quantity in the diabatic representation by expressing it in terms of the adiabatic-to-diabatic transform angle and the basic vectors of the adiabatic quantities, including the off-diagonal matrix element and the difference in the diagonal matrix elements. By using a general vector observable, which might be detected experimentally or estimated theoretically, the equation can be applied to transforming information between adiabatic and diabatic representations. We have also deduced all possible trajectories of the diabatic quantity for systems with different features. The trajectory is located on the same line as the non-zero basic vector, when one of the basic vectors vanishes. In general, however, the trajectory is an ellipse as the adiabatic-to-diabatic transformation angle θ varies, when the two basic vectors form either an orthogonal or an oblique coordinate system. For different cases, we have discussed the extremes of the diabatic transition. The results show that both the direction and the magnitudes of the two adiabatic basic vectors should be taken into consideration, for the purpose of evaluating the diabatic transition accurately from the adiabatic-to-diabatic transformation angle, and vice versa. Meanwhile, forcing the diabatic transition to take vanishing value will unavoidably introduce some sorts of deviations. Because the pilot implementation of the analysis with the approximated diabatic transition dipole produces electronic coupling about the same as the GMH method for the testing molecule, we infer that the analysis is appropriate for addressing the adiabatic-to-diabatic transformation issue.

To the best of our knowledge, this is the first time that the adiabatic-to-diabatic transformation is carried out in a more general two-dimensional scale by means of applying both the magnitude and the direction of the two basic adiabatic qualities of a physical observable. The transformation scheme may provide an efficient way to evaluate diabatic qualities from the adiabatic ones. This analysis lays the mathematical foundation for the adiabatic-to-diabatic transformation via the assistance of a physical observable. Because the physical observable in this work is completely general, many properties such as the dipole moment, polarizability, electromagnetic susceptibility, etc. are free for us to select depending on the convenience of the actual measurements. Consequently, our analysis may have a broad range of applications.

■ ASSOCIATED CONTENT

Supporting Information

The Supporting Information is available free of charge on the ACS Publications website at DOI: 10.1021/acs.jpclett.9b01812.

DOI: 10.1021/acs.jpclett.9b01812
J. Phys. Chem. Lett. 2019, 10, 5868−5872

Evaluation of the approximate diabatic transition dipole moment and the data for Figure 4 (PDF)

■ AUTHOR INFORMATION

Corresponding Author

*E-mail: zhhchen@xmu.edu.cn. Fax: (86)592-2184708.

ORCID

Zhenhua Chen: 0000-0001-5545-4462

Wei Wu: 0000-0002-6139-5443

Notes

The authors declare no competing financial interest.

■ ACKNOWLEDGMENTS

This project is supported by the Natural Science Foundation of China (21733008 and 21673186).

■ REFERENCES

(1) Hyeon-Deuk, K.; Kim, J.; Prezhdo, O. V. Ab Initio Analysis of Auger-Assisted Electron Transfer. *J. Phys. Chem. Lett.* **2015**, *6*, 244−249.

(2) Long, R.; Fang, W.; Prezhdo, O. V. Moderate Humidity Delays Electron−Hole Recombination in Hybrid Organic−Inorganic Perovskites: Time-Domain Ab Initio Simulations Rationalize Experiments. *J. Phys. Chem. Lett.* **2016**, *7*, 3215−3222.

(3) Long, R.; Fang, W.; Akimov, A. V. Nonradiative Electron−Hole Recombination Rate Is Greatly Reduced by Defects in Monolayer Black Phosphorus: Ab Initio Time Domain Study. *J. Phys. Chem. Lett.* **2016**, *7*, 653−659.

(4) Pramod, P.; Soumya, C. C.; Thomas, K. G. Gold Nanoparticle-Functionalized Carbon Nanotubes for Light-Induced Electron Transfer Process. *J. Phys. Chem. Lett.* **2011**, *2*, 775−781.

(5) Yarkony, D. R. Nonadiabatic Quantum Chemistry—Past, Present, and Future. *Chem. Rev.* **2012**, *112*, 481−498.

(6) Tully, J. C. Perspective: Nonadiabatic dynamics theory. *J. Chem. Phys.* **2012**, *137*, 22A301.

(7) Crespo-Otero, R.; Barbatti, M. Recent Advances and Perspectives on Nonadiabatic Mixed Quantum−Classical Dynamics. *Chem. Rev.* **2018**, *118*, 7026−7068.

(8) Kim, W.; Sung, J.; Grzybowski, M.; Gryko, D. T.; Kim, D. Modulation of Symmetry-Breaking Intramolecular Charge-Transfer Dynamics Assisted by Pendant Side Chains in π-Linkers in Quadrupolar Diketopyrrolopyrrole Derivatives. *J. Phys. Chem. Lett.* **2016**, *7*, 3060−3066.

(9) Matsuoka, T.; Takatsuka, K. Dynamics of photoionization from molecular electronic wavepacket states in intense pulse laser fields: A nonadiabatic electron wavepacket study. *J. Chem. Phys.* **2017**, *146*, 134114.

(10) Chaudhuri, S.; Acharya, A.; Nibbering, E. T. J.; Batista, V. S. Regioselective Ultrafast Photoinduced Electron Transfer from Naphthols to Halocarbon Solvents. *J. Phys. Chem. Lett.* **2019**, *10*, 2657−2662.

(11) Gray, H. B.; Winkler, J. R. Electron Transfer in Proteins. *Annu. Rev. Biochem.* **1996**, *65*, 537−561.

(12) Winkler, J. R.; Gray, H. B. Electron Flow through Metalloproteins. *Chem. Rev.* **2014**, *114*, 3369−3380.

(13) Farver, O.; Hosseinzadeh, P.; Marshall, N. M.; Wherland, S.; Lu, Y.; Pecht, I. Long-Range Electron Transfer in Engineered Azurins Exhibits Marcus Inverted Region Behavior. *J. Phys. Chem. Lett.* **2015**, *6*, 100−105.

(14) Li, S. L.; Xu, X.; Hoyer, C. E.; Truhlar, D. G. Nonintuitive Diabatic Potential Energy Surfaces for Thioanisole. *J. Phys. Chem. Lett.* **2015**, *6*, 3352−3359.

(15) Joubert-Doriol, L.; Sivasubramanium, J.; Ryabinkin, I. G.; Izmaylov, A. F. Topologically Correct Quantum Nonadiabatic Formalism for On-the-Fly Dynamics. *J. Phys. Chem. Lett.* **2017**, *8*, 452−456.

(16) Zhu, X.; Yarkony, D. R. Fitting coupled potential energy surfaces for large systems: Method and construction of a 3-state representation for phenol photodissociation in the full 33 internal degrees of freedom using multireference configuration interaction determined data. *J. Chem. Phys.* **2014**, *140*, 024112.

(17) Lichten, W. Molecular Wave Functions and Inelastic Atomic Collisions. *Phys. Rev.* **1967**, *164*, 131−142.

(18) Smith, F. T. Diabatic and Adiabatic Representations for Atomic Collision Problems. *Phys. Rev.* **1969**, *179*, 111−123.

(19) O'Malley, T. F. Diabatic States of Molecules: Quasistationary Electronic States. In *Advances in Atomic and Molecular Physics*; Bates, D. R., Esterman, I., Eds.; Academic Press, 1971.

(20) Ruedenberg, K.; Atchity, G. J. A quantum chemical determination of diabatic states. *J. Chem. Phys.* **1993**, *99*, 3799−3803.

(21) Nakamura, H.; Truhlar, D. G. The direct calculation of diabatic states based on configurational uniformity. *J. Chem. Phys.* **2001**, *115*, 10353−10372.

(22) Wu, Q.; Van Voorhis, T. Extracting electron transfer coupling elements from constrained density functional theory. *J. Chem. Phys.* **2006**, *125*, 164105.

(23) Van Voorhis, T.; Kowalczyk, T.; Kaduk, B.; Wang, L.-P.; Cheng, C.-L.; Wu, Q. The diabatic picture of electron transfer, reaction barriers, and molecular dynamics. *Annu. Rev. Phys. Chem.* **2010**, *61*, 149−170.

(24) Wu, W.; Su, P.; Shaik, S.; Hiberty, P. C. Classical Valence Bond Approach by Modern Methods. *Chem. Rev.* **2011**, *111*, 7557−7593.

(25) Lin, X.; Liu, X.; Ying, F.; Chen, Z.; Wu, W. Explicit construction of diabatic state and its application to the direct evaluation of electronic coupling. *J. Chem. Phys.* **2018**, *149*, 044112.

(26) Baer, M. Adiabatic and diabatic representations for atom-molecule collisions: Treatment of the collinear arrangement. *Chem. Phys. Lett.* **1975**, *35*, 112−118.

(27) Halász, G. J.; Vibók, A.; Suhai, S.; Baer, M. The electronic nonadiabatic coupling term: Can it be ignored in dynamic calculations? *J. Chem. Phys.* **2007**, *127*, 244101.

(28) Creutz, C.; Newton, M. D.; Sutin, N. Metal—lingad and metal—metal coupling elements. *J. Photochem. Photobiol., A* **1994**, *82*, 47−59.

(29) Cave, R. J.; Newton, M. D. Generalization of the Mulliken-Hush treatment for the calculation of electron transfer matrix elements. *Chem. Phys. Lett.* **1996**, *249*, 15−19.

(30) Subotnik, J. E.; Yeganeh, S.; Cave, R. J.; Ratner, M. A. Constructing diabatic states from adiabatic states: Extending generalized Mulliken−Hush to multiple charge centers with Boys localization. *J. Chem. Phys.* **2008**, *129*, 244101.

(31) Hoyer, C. E.; Xu, X.; Ma, D.; Gagliardi, L.; Truhlar, D. G. Diabatization based on the dipole and quadrupole: the DQ method. *J. Chem. Phys.* **2014**, *141*, 114104.

(32) Hoyer, C. E.; Parker, K.; Gagliardi, L.; Truhlar, D. G. The DQ and DQΦ electronic structure diabatization methods: Validation for general applications. *J. Chem. Phys.* **2016**, *144*, 194101.

(33) Voityuk, A. A.; Rosch, N. Fragment charge difference method for estimating donor−acceptor electronic coupling: Application to DNA -stacks. *J. Chem. Phys.* **2002**, *117*, 5607−5616.

(34) Hsu, C.-P. The Electronic Couplings in Electron Transfer and Excitation Energy Transfer. *Acc. Chem. Res.* **2009**, *42*, 509−518.

(35) Varga, Z.; Parker, K. A.; Truhlar, D. G. Direct diabatization based on nonadiabatic couplings: the N/D method. *Phys. Chem. Chem. Phys.* **2018**, *20*, 26643−26659.

(36) Mulliken, R. S. Molecular compounds and their spectra. II. *J. Am. Chem. Soc.* **1952**, *74*, 811−824.

(37) Hush, N. S. Homogeneous and heterogeneous optical and thermal electron transfer. *Electrochim. Acta* **1968**, *13*, 1005−1023.

(38) Werner, H. J.; Meyer, W. MCSCF study of the avoided curve crossing of the two lowest $^1\Sigma^+$ states of LiF. *J. Chem. Phys.* **1981**, *74*, 5802−5807.

(39) Kryachko, E. S.; Yarkony, D. R. Diabatic bases and molecular properties. *Int. J. Quantum Chem.* **2000**, *76*, 235−243.

DOI: 10.1021/acs.jpclett.9b01812
J. Phys. Chem. Lett. 2019, 10, 5868−5872